ELSEVIER

Immunohistochemical, in situ hybridization, and ultrastructural localization of SARS-associated coronavirus in lung of a fatal case of severe acute respiratory syndrome in Taiwan

Wun-Ju Shieh MD, MPH, PhD[a], Cheng-Hsiang Hsiao MD[b], Christopher D. Paddock MD[a], Jeannette Guarner MD[a], Cynthia S. Goldsmith MS[a], Kathleen Tatti PhD[a], Michelle Packard MPH[a], Laurie Mueller BA, BS[a], Mu-Zong Wu[b], Pierre Rollin MD[c], Ih-Jen Su MD, PhD[d], Sherif R. Zaki MD, PhD[a],*

[a]Infectious Disease Pathology Activity, Division of Viral and Rickettsial Diseases, Centers for Disease Control and Prevention, Atlanta, GA 30333, USA
[b]Department of Pathology, National Taiwan University Hospital, Taipei, Republic of China
[c]Special Pathogens Branch, Division of Viral and Rickettsial Diseases, Centers for Disease Control and Prevention, Atlanta, GA, USA
[d]Center for Disease Control, Taiwan, Republic of China

Summary This article describes the pathological studies of fatal severe acute respiratory syndrome (SARS) in a 73-year-old man during an outbreak of SARS in Taiwan, 2003. Eight days before onset of symptoms, he visited a municipal hospital that was later identified as the epicenter of a large outbreak of SARS. On admission to National Taiwan University Hospital in Taipei, the patient experienced chest tightness, progressive dyspnea, and low-grade fever. His condition rapidly deteriorated with increasing respiratory difficulty, and he died 7 days after admission. The most prominent histopathologic finding was diffuse alveolar damage of the lung. Immunohistochemical and in situ hybridization assays demonstrated evidence of SARS-associated coronavirus (SARS-CoV) infection in various respiratory epithelial cells, predominantly type II pneumocytes, and in alveolar macrophages in the lung. Electron microscopic examination also revealed coronavirus particles in the pneumocytes, and their identity was confirmed as SARS-CoV by immunogold labeling electron microscopy. This report is the first to describe the cellular localization of SARS-CoV in human lung tissue by using a combination of immunohistochemistry, double-stain immunohistochemistry, in situ hybridization, electron microscopy, and immunogold labeling

 * Corresponding author.
 E-mail address: sZaki@cdc.gov (S.R. Zaki).

electron microscopy. These techniques represent valuable laboratory diagnostic modalities and provide insights into the pathogenesis of this emerging infection.

1. Introduction

Severe acute respiratory syndrome (SARS) is an emergent respiratory viral disease that was first reported in Asia during February 2003 and quickly spread to many countries in North and South America, Europe, and Asia. Through December 2003, this global epidemic had resulted in 8098 reported probable cases, of which 774 were fatal [1]. Various reports have described diffuse alveolar damage as the main histopathologic finding in patients with SARS [2-4], and SARS-associated coronavirus (SARS-CoV) has been demonstrated in human and experimental animal tissues by immunohistochemical or in situ hybridization (ISH) assays [5-12]. Coronavirus-like particles have been detected by electron microscopy (EM) in cells from a bronchoalveolar lavage specimen [4,13] and in pneumocytes from postmortem lung samples [2,6]. Because coronavirus particles may be confused morphologically with other nonviral cellular components, a specific technique, such as immunogold labeling EM (IEM), is needed to definitively characterize SARS-CoV particles. We describe the use of immunohistochemistry (IHC), ISH, EM, and IEM for the pathological diagnosis of SARS and cellular localization of SARS-CoV. We also discuss the use of these techniques to investigate the pathogenesis of this emerging infection.

2. Case report

This 73-year-old male patient sought medical treatment at the emergency service at National Taiwan University Hospital (NTUH) in Taipei, Taiwan, on April 23, 2003, because of recurrent dyspnea and orthopnea. His past medical history included 3 years of type 2 diabetes mellitus, a myocardial infarct 2 years earlier, and 2 recent admissions to NTUH due to acute coronary syndrome and congestive heart failure.

On arrival at emergency service, the patient was afebrile and initial physical examination revealed a temperature of 37°C, heart rate of 112 beats per minute, and respiration rate of 24/min. Chest x-ray showed mild pulmonary congestion. The temperature elevated to 37.9°C 2 hours later, and urinalysis showed 20 to 30 white blood cells. A presumptive diagnosis of urinary tract infection and congestive heart failure was made, and the patient was treated with antibiotics, diuretics, and intravenous nitroglycerin. The patient was admitted to a cardiology ward 2 days later and became increasingly dyspneic with a nonproductive cough and persistent low-grade fever. Serial chest x-rays showed progressive lung infiltrates. A more detailed history revealed that the patient had visited Taipei Hoping City Hospital on April 15 and 16. Because this hospital was associated with a large nosocomial outbreak of SARS during late April, the patient was immediately isolated as a probable SARS case. Throat and nasopharyngeal swabs were positive for SARS-CoV by viral isolation and polymerase chain reaction (PCR) assay. He was transferred to an intensive care unit on April 29 after sudden onset of mental status changes, hypotension, and melena. The patient subsequently developed ventricular fibrillation and died 1 day later.

3. Materials and methods

Lung tissues obtained from a limited autopsy were fixed in 10% buffered formalin and paraffin embedded. Tissue sections were stained by routine hematoxylin and eosin for histopathologic evaluation.

Immunohistochemistry was performed as previously described [14] by using a colorimetric indirect immunoalkaline phosphatase method with a hyperimmune mouse anti–SARS-CoV ascitic fluid. Negative controls included Vero E6 cells infected with human coronavirus OC43, Vero E6 cells infected with human coronavirus 229E, noninfected Vero cells, and tissues from non-SARS cases. Normal mouse antiserum was used as a negative control antibody. Double-stain IHC was performed by using peroxidase polymer (DAKO, Carpinteria, CA)–labeled antibodies against cytokeratin, surfactant, or CD68 (DAKO), followed by the mouse anti–SARS-CoV antibody labeled with immunoalkaline phosphatase polymer.

A colorimetric ISH was performed as previously described [14]. Briefly, negative-sense digoxin-labeled riboprobes were generated from PCR products amplified from the nucleocapsid (N) (625 bases in length) or polymerase (Pol) (325 bases in length) regions of the SARS-CoV genome and tailed with the T7 promoter. Tissue sections were incubated with a pool of N and Pol probes.

Specimens for EM were excised from paraffin-embedded blocks of lung in areas corresponding to positive IHC and ISH results. Tissues were deparaffinized in xylene and embedded for EM as previously described [13]. Immunogold labeling assays used the same mouse anti–SARS-CoV antibody as IHC experiments, and the antibody was detected by using goat antimouse conjugated to 12-nm colloidal gold.

4. Results

4.1. Histopathology

The lungs showed features characteristic of the proliferative phase of diffuse alveolar damage, with

desquamation of epithelial cells, fibrin deposits in the alveolar spaces, hyperplasia of type II pneumocytes, and increased mononuclear inflammatory cell infiltrates in the interstitium (Fig. 1A). No multinucleated syncytial cells were observed.

4.2. Immunohistochemistry

SARS-CoV antigens were abundant and distributed multifocally in the lung. Viral antigens were seen predominantly in the cytoplasm of pneumocytes (Fig. 1B and C),
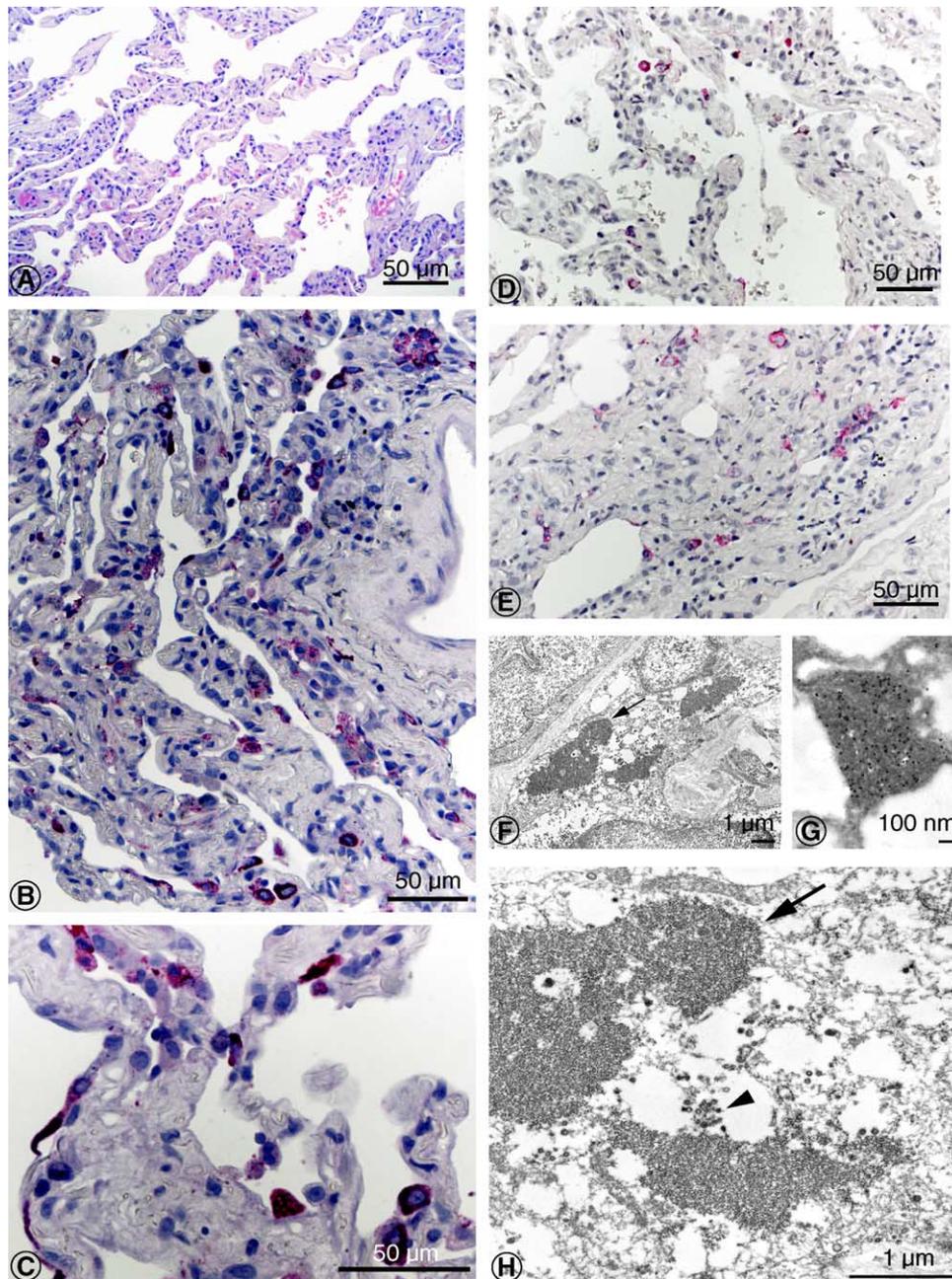

Fig. 1   A, Histopathology of lung from SARS patient showed diffuse alveolar damage, characterized by desquamation of epithelial cells, fibrin deposits in the alveolar space, hyperplasia of type II pneumocytes, and increased mononuclear infiltrate in the interstitium (hematoxylin and eosin stain). B and C, SARS-CoV antigens in pneumocytes (immunoalkaline phosphatase with naphthol fast-red substrate and hematoxylin counterstain). D and E, SARS-CoV nucleic acids in pneumocytes (ISH with naphthol fast-red substrate and hematoxylin counterstain). F and H, SARS-CoV–infected interstitial cell, with viral nucleocapsid inclusion bodies (arrows) and virions in cellular vesicles (arrowhead). G, SARS-CoV antigens were detected within the cytoplasmic inclusions (immunogold labeling with 12-nm colloidal gold). Bar size indicated in micrometers and nanometers.

occasionally in macrophages, and in association with intraalveolar necrotic debris. Double staining revealed that most infected cells were pneumocytes (colabeled with cytokeratin, Fig. 2A), predominantly type II pneumocytes (colabeled with surfactant, Fig. 2B), and less frequently macrophages (colabeled with CD68, Fig. 3A). Negative controls did not show staining by IHC with anti–SARS-CoV antibody. Normal mouse antiserum did not show any staining on SARS-CoV–infected Vero cells and lung tissues of this case.

4.3. In situ hybridization

Viral nucleic acids were detected by ISH with a distribution similar to that identified by using IHC, mainly in pneumocytes and some macrophages (Fig. 1D and E). All
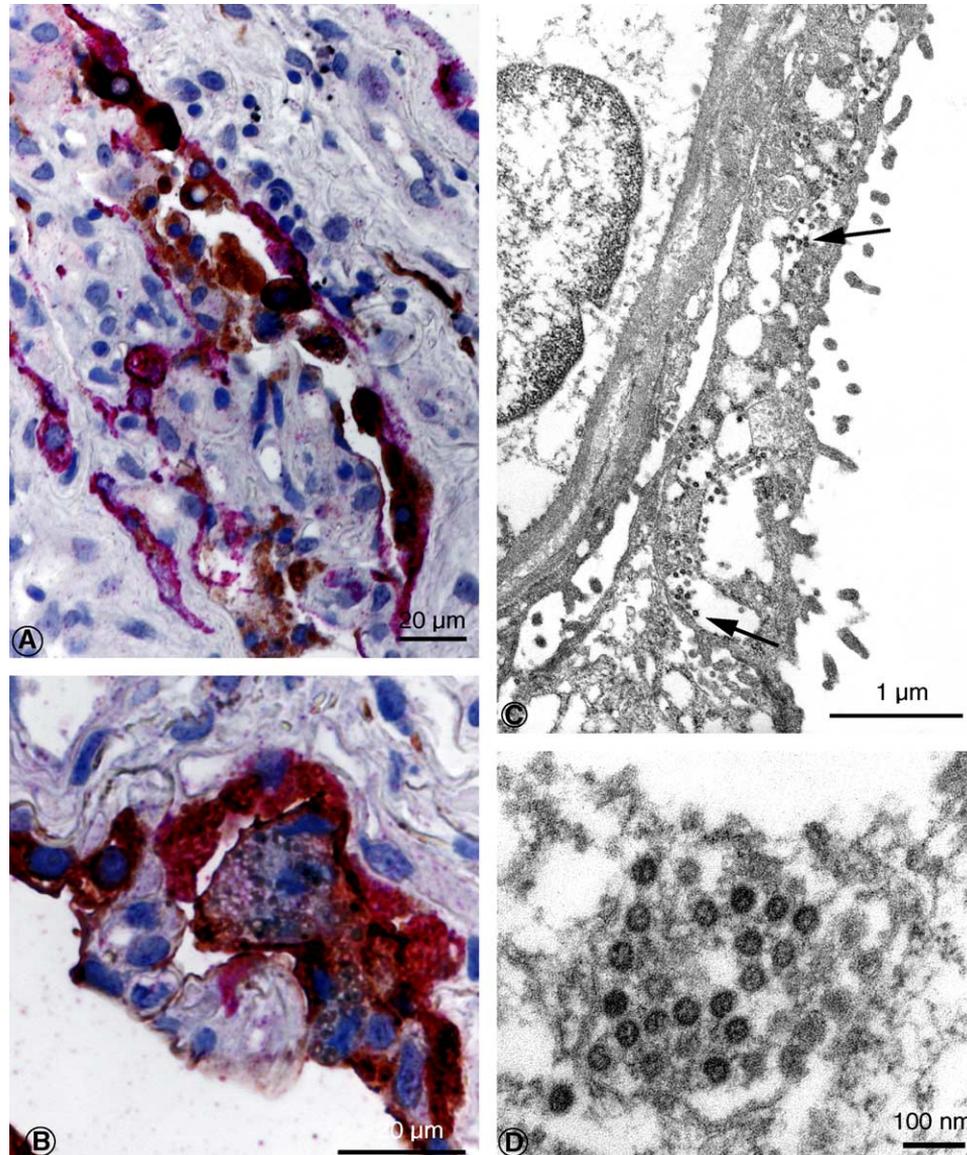

Fig. 2   A, SARS-CoV and cytokeratin antigens in pneumocytes. Red stain, SARS-CoV; brown stain, cytokeratin (double-stain IHC immunoalkaline phosphatase polymer and with peroxidase polymer). B, SARS-CoV and surfactant antigens in type II pneumocytes. Red stain, SARS-CoV; brown stain, surfactant (double-stain IHC with immunoalkaline phosphatase polymer and peroxidase polymer). C, Numerous virions (arrows) are seen within the cytoplasmic vesicles of this pneumocyte, overlying the basement membrane and another pneumocyte. D, SARS-CoV particles, averaging 51 nm in these deparaffinized tissues, are seen in a cytoplasmic vesicle of an infected pneumocyte. Virions are composed of a helical nucleocapsid, often seen in cross section, surrounded by a viral envelope. Bar size indicated in micrometers and nanometers.
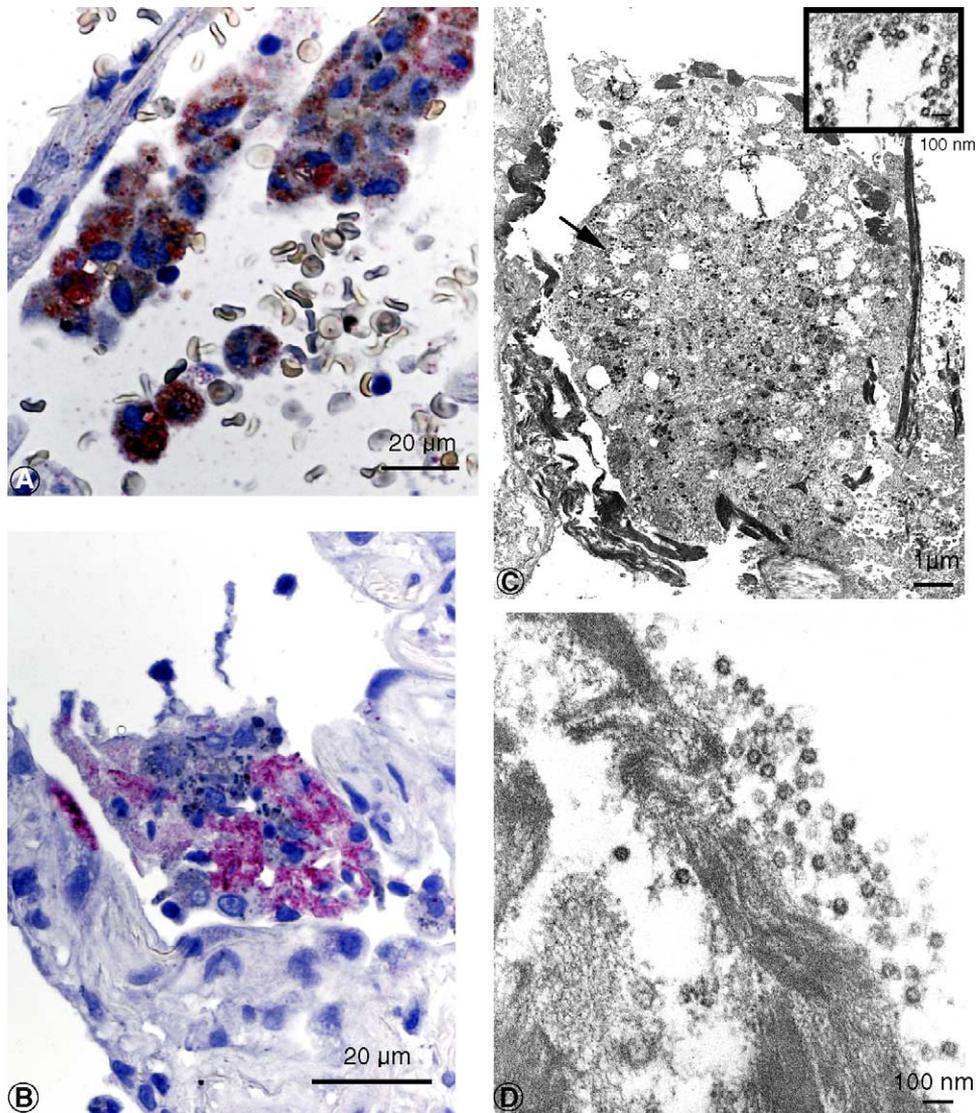
Fig. 3   A, SARS-CoV and CD68 antigens in alveolar macrophage. Red stain, SARS-CoV; brown stain, CD68 (double-stain IHC with immunoalkaline phosphatase and peroxidase polymer). B, SARS-CoV antigens in intraalveolar necrotic debris. C and D, Extracellular virions were often associated with fibrin within the alveolar space. C inset, Higher magnification of area at arrow. Bar size indicated in micrometers or nanometers.

pertinent positive and negative controls were run in parallel with comparable results described for IHC.

4.4. Electron microscopy

Electron microscopy examination of lung tissues that had been selected from areas with abundant IHC staining showed numerous viral particles and nucleocapsid inclusions typical of the family Coronaviridae. Virions were predominantly seen in cytoplasmic vesicles (Figs. 1F, H and 2C, D) and along the cell membranes of pneumocytes, which were attached to the basement membrane or free in the alveolar space, in phagosomes of macrophages (Fig. 3C and inset), and associated with fibrin in alveolar spaces (Fig. 3D). Some

infected cells also had prominent coronavirus nucleocapsid inclusions (Fig. 1F and H). The viral nature of the observed particles and cytoplasmic inclusions was confirmed by IEM labeling (Fig. 1G).

5. Discussion

In this report, we describe the localization of SARS-CoV in various cellular and extracellular locations in the lung of a patient who died of SARS. Previous studies have demonstrated the cellular tropism of SARS-CoV in the tissues of patients by using ISH [5,7,11,12] or EM [2,4,13,15]. Immunohistochemical has also been used to

localize viral antigens in the human tissues [12] and tissues of animals experimentally infected with SARS-CoV [6,8-10]. To our knowledge, this is the first report to localize SARS-CoV in human tissues by using IEM and double-stain IHC. In an earlier study of 4 human cases [4], we were not able to demonstrate viral antigens in the lung by IHC. The most likely explanation is that all tissue samples from patients in that study were obtained after a clinical course lasting longer than 14 days. In a recent report by Chong et al [7], a similar observation was documented with the inability of ISH to detect viral nucleic acids in patients who died beyond 8 days. The patient in this case report died 7 days after onset of symptoms, and coronavirus antigens and RNA could be detected by IHC and ISH. Electron microscopy also identified viral particles in the lung tissue, and the viral nature of these particles was confirmed by IEM. More cases are needed to further characterize the temporal relationship between the duration of illness and viral clearance in human lung tissue.

The development of a specific IHC, ISH, and IEM to identify SARS-CoV in formalin-fixed, paraffin-embedded samples also allowed us to assess the cellular tropism of SARS-CoV infection in human lung tissues. SARS-CoV antigens were localized primarily in the cytoplasm of type II pneumocytes, and occasionally in alveolar macrophages. Type II pneumocytes are known to secrete pulmonary surfactant, which reduces surface tension and preserves the integrity of the alveolar space. These cells also play an important role in tissue restitution after lung damage. There is also mounting evidence to support their contribution to the development of acute inflammatory lung injury after exposure to biological or chemical agents. Type II pneumocytes can be directly infected by bacteria or viruses and modulate the corresponding pathogenesis of these organisms. Additional studies are needed to further define the role of type II pneumocytes and alveolar macrophages in SARS-CoV infection. Haagmans et al [10] showed extensive SARS-CoV antigen expression in experimentally infected cynomolgus macaques at day 4 postinfection. The antigens were mainly in alveolar lining epithelial cells with morphologic characteristics of type I pneumocytes, suggesting that type I pneumocytes are the primary targets for SARS-CoV infection early in the disease. In a recent study using a nonhuman primate model [8], we examined the lung tissues of day 2 postinfection monkeys and demonstrated that type I pneumocytes were the main type of cells involved at this early stage, whereas only some type II pneumocytes were involved. Type I pneumocytes normally represent 90% of the alveolar epithelial cell volume and are easily damaged during pulmonary infections or other types of injury. Type II pneumocytes are more resistant to damage, and this feature is important for the repair process because these cells produce surfactant, proliferate, and differentiate into type I cells during lung damage. Collectively, these data indicate that SARS-CoV infects both type I and II pneumocytes, and clearance and localization of the virus may depend on the stage of illness as well as individual immunologic responses. Other target cells for SARS-CoV infection, such as bronchiolar epithelial cells [14], may also have a significant role in virus replication and transmission.

The emergence of SARS-CoV has posed a major threat to global health. A specific etiologic diagnosis is particularly important during SARS-CoV disease outbreaks because of the impact on hospital infection control and other public health measures. Because the clinical features of SARS-CoV infection can be similar to those of many other respiratory infections, a definitive diagnosis can be made only by laboratory confirmation. Laboratory assays currently used for SARS diagnosis include virus isolation, PCR, and serology. Pathology-based methods, such as IHC, ISH, EM, and IEM, offer the advantage of interpreting the test results within a morphologic context and can also be used for diagnosis if appropriate tissue specimens are available. Despite the limited tissue samples in this single case report, we were able to successfully use specific IHC, ISH, and IEM methods for SARS-CoV detection in human lung tissue. These methods should help enhance the pathological diagnosis and further our understanding of the pathogenesis of SARS-CoV infection.

References

[1] WHO issues consensus document on the epidemiology of SARS. Wkly Epidemiol Rec 2003;78:373-5.

[2] Nicholls JM, Poon LL, Lee KC, et al. Lung pathology of fatal severe acute respiratory syndrome. Lancet 2003;361(9371):1773-8.

[3] Franks TJ, Chong PY, Chui P, et al. Lung pathology of severe acute respiratory syndrome (SARS): a study of 8 autopsy cases from Singapore. Hum Pathol 2003;34(8):743-8.

[4] Ksiazek TG, Erdman D, Goldsmith CS, et al. A novel coronavirus associated with severe acute respiratory syndrome. N Engl J Med 2003;348(20):1953-66.

[5] Nakajima N, Asahi-Ozaki Y, Nagata N, et al. SARS coronavirus-infected cells in lung detected by new in situ hybridization technique. Jpn J Infect Dis 2003;56(3):139-41.

[6] Kuiken T, Fouchier RA, Schutten M, et al. Newly discovered coronavirus as the primary cause of severe acute respiratory syndrome. Lancet 2003;362(9380):263-70.

[7] Chong PY, Chui P, Ling AE, et al. Analysis of deaths during the severe acute respiratory syndrome (SARS) epidemic in Singapore: challenges in determining a SARS diagnosis. Arch Pathol Lab Med 2004;128(2):195-204.

[8] McAuliffe J, Vogel L, Roberts A, et al. Replication of SARS coronavirus administered into the respiratory tract of African green, rhesus and cynomolgus monkeys. Virology 2004;330:8-15.

[9] Roberts A, Vogel L, Guarner J, et al. SARS coronavirus infection of golden syrian hamsters. J Virol 2005;79:503-11.

[10] Haagmans BL, Kuiken T, Martina BE, et al. Pegylated interferon-alpha protects type 1 pneumocytes against SARS coronavirus infection in macaques. Nat Med 2004;10(3):290-3.

[11] To KF, Tong JH, Chan PK, et al. Tissue and cellular tropism of the coronavirus associated with severe acute respiratory syndrome: an in-situ hybridization study of fatal cases. J Pathol 2004;202(2):157-63.

[12] Ding Y, He L, Zhang Q, et al. Organ distribution of Severe Acute Respiratory Syndrome (SARS) Associated Coronavirus (SARS-CoV) in SARS patients: implications for pathogenesis and virus transmission pathways. J Pathol 2004;203(2):622-30.

[13] Goldsmith CS, Tatti KM, Ksiazek TG, et al. Ultrastructural characterization of SARS coronavirus. Emerg Infect Dis 2004;10(2):320-6.

[14] Subbarao K, McAuliffe J, Vogel L, et al. Prior infection and passive transfer of neutralizing antibody prevent replication of severe acute respiratory syndrome coronavirus in the respiratory tract of mice. J Virol 2004;78(7):3572-7.

[15] Peiris JS, Lai ST, Poon LL, et al. Coronavirus as a possible cause of severe acute respiratory syndrome. Lancet 2003;361(9366):1319-25.